Journal of Manufacturing Processes 69 (2021) 142–151

Contents lists available at ScienceDirect

Journal of Manufacturing Processes

journal homepage: www.elsevier.com/locate/manpro

Simulated thermal tests of a molybdenum/graphite X-ray target manufactured with a novel Ti-Zr-Nb-Be powder filler metal: an investigation of the brazed joint evolution under operating conditions

Ivan Fedotov [a,*], Alexey Suchkov [a], Andrey Sliva [b], Pavel Dzhumaev [a], Ilya Kozlov [a,c], Roman Svetogorov [c], Oleg Sevryukov [a]

[a] National Research Nuclear University MEPhI (Moscow Engineering Physics Institute), Moscow, 115409 Russia
[b] National Research University "Moscow Power Engineering Institute", Moscow, 111250 Russia
[c] National Research Center "Kurchatov Institute", Moscow, 123182 Russia

ARTICLE INFO

Keywords:
Brazing
Molybdenum
Graphite
Joining
Anode
Shear strength

ABSTRACT

In this work, two molybdenum-graphite X-ray targets for computed tomography/angiography devices were manufactured with usage of Ti-40Zr-8.5Nb-1.5Be filler metal and 1400 °C – 20 min brazing mode. To confirm the efficiency of the proposed brazing method, a mechanical test and simulated heating of the anodes were carried out, as well as a study of the evolution of the brazed joint under operating conditions. The brazed joint of the anodes showed stability and maintained integrity after tests. However, it is revealed that the long-term heat treatment of the brazed Mo/graphite joint leads to an increase in the amount of carbides in the seam, and also converts the seam into a refractory state by suppressing the formation of beryllium eutectic, while the cyclic heating mainly affects the recrystallization of the seam phases, leading to phase fragmentation. Shear strength tests after simulated heating show that the failure of the Mo/graphite joint occurs in the graphite element with cracking due to the infiltration of the filler metal into graphite through the open porosity. Infiltrates could provoke the occurrence of stresses during cyclic heating/cooling because of the difference in the CTE of graphite and carbide phases. Nevertheless, the joints remained integrity and showed a minimal strength of 23.4 ± 2.5 MPa (after 20 heating cycles of 350 ↔ 1400 °C) and 26.1 ± 6.4 MPa (after vacuum annealing of 1400 °C – 8 h).

1. Introduction

In medicine, computed tomography and angiography are used to examine the blood vessels and tissues of the human body. The manufacture of such complex medical equipment requires the use of special materials, which work in a complex thermally stressed state, almost at the limit of their capabilities. The main energy-stressed element in such radiographic devices is an X-ray tube. In high-power X-ray tubes, the main body of the target is produced in the form of a disk with a diameter from 60 to 238 mm made of a molybdenum alloy with W-Re coating and a brazed graphite backed heat accumulator, which also acts as a radiation heat dissipator [1]. Currently, molybdenum or its alloy – TZM (Mo-0.5Ti-0.1Zr-0.02C w.p.) can be combined with graphite with usage of various filler metals, including Cu-1Cr, Ag-27Cu-3Ti, Cu-10Ti, Ni-10Ti [2,3] or alloys of the Ni-Cr, Ti-Zr binary system [4,5]. However, the filler metals based on copper, silver or nickel cannot be used for manufacturing a heat-resistant Mo/graphite brazed joint, since these elements have a low melting point and do not form refractory carbides. The accumulation of these elements in the brazed seam will lead to secondary melting under the operating conditions of the X-ray target. Thus, the most common method of manufacturing molybdenum-graphite targets for X-ray tubes is currently contact-reactive brazing with pure zirconium [6,7] at high (1600–2000 °C) temperatures, which ensures the formation of refractory zirconium carbide and Zr-Mo_2Zr eutectic with a high melting point in the seam. But a high brazing temperature can lead to degradation of the mechanical properties of molybdenum or the TZM alloy [8,9]. In order to decrease the degradation of metal disk mechanical properties, a method of two-stage X-ray target manufacturing can be used [10]. At the first stage, a thin molybdenum plate joins a graphite disk by contact-reactive brazing with zirconium. At the second stage, with usage of Ti-25Cr-3Be or Ti-8.5Si filler metals and brazing temperatures of about 1200 °C, the plate is

* Corresponding author.
E-mail address: IVFedotov@mephi.ru (I. Fedotov).

https://doi.org/10.1016/j.jmapro.2021.07.035
Received 25 May 2021; Received in revised form 15 July 2021; Accepted 15 July 2021
Available online 28 July 2021

connected to a metal main body disk. Lower brazing temperatures prevent degradation of the molybdenum disk mechanical properties and reduce residual thermal stresses, which improves reliability and extends the service life of the X-ray tube. However, this process is quite complicated, since it requires more procedures compared to single-stage brazing.

In the previous work, a powder filler metal Ti-40Zr-8.5Nb-1.5Be wt %, made of a rapidly quenched tape, was developed for the molybdenum/graphite joining [11]. The developed filler metal mainly contains elements that can form refractory carbides (TiC, ZrC, NbC), which is necessary to obtain a Mo/graphite joint, that can withstand high temperatures. The main role of the beryllium additive in the filler metal was to reduce the melting point and the brazing temperature. A lower brazing temperature has a favorable effect by reducing the molybdenum recrystallization degree and reducing post-brazing residual thermal stresses. Previously, it has been shown, that the application of Ti-40Zr-8.5Nb-1.5Be filler metal is promising for the manufacture of X-ray targets at a reduced (1400 °C) brazing temperature. Rapidly quenched filler metals show excellent results when used for high-temperature applications [12–14]. However, since such alloys contain elements that are contributing to amorphization, there is a risk of brittle intermetallic compounds forming in the brazed joint. Therefore, the actual use of the developed brazing technology requires a complex set of experiments confirming the performance of the X-ray target, including the temperature conditions imitation and the investigation of the brazing seam microstructure evolution. Several works show that the brazed seam of a molybdenum disk/graphite heat accumulator works in a gradient thermal field. At the periphery of the X-ray target, the temperature of the brazed seam can reach 1400 °C during normal operation and up to 1500 °C during the exhaust process [15,16]. Typical conditions for a brazed seam in such a product are thermal cycling from the range of 350–450 °C (warm start) to 1350–1400 °C with a heating time of 10–30 s. This thermal cyclic load strongly effects the microstructure of the brazed seam and its mechanical properties. Several authors note that post-brazing heating of the brazed joint can cause the formation and growth of the fragile phases in a seam, which reduce the strength of the joint [17–19]. The “shock” heating can also be very dangerous for brazed joints of brittle materials, such as graphite and ceramics, since it can lead to the formation and growth of cracks in the base material or/and the residual stress accumulation due to the penetration of the filler metal into the open porosity [20–22]. Thus, the study of the “shock” heating effect on the microstructure and properties of brazed joints is relevant for energy-stressed equipment, since a decrease in the strength of the joint or softening of the base material under operating conditions can lead to failure.

The aim of this work was the experimental brazing of X-ray targets with a novel Ti-40Zr-8.5Nb-1.5Be filler metal, as well as an investigation of the brazed joint evolution under different heating conditions. The results of this work can be useful in studying the effect of thermal load on the evolution of the brazed seam microstructure and its mechanical properties for energy-stressed equipment and become another step towards the implementation of the proposed brazing method for the manufacturing of X-ray targets.

2. Materials and experimental procedures

2.1. Brazing of X-ray targets and samples of Mo/graphite joint

Commercial molybdenum with Mo purity >99.9 wt% and graphite of the MPG-6 grade were used as initial materials. The MPG-6 grade graphite is a widely used material, that can be used in energy-stressed equipment with good thermal and mechanical properties: density of at least 1.6 g/sm^3, thermal conductivity >94 W/m · °K and heat capacity >0.7 kJ/kg · °K [23,24]. In this work, two anodes of an X-ray tube with diameters of 100 and 120 mm were manufactured, as shown in Fig. 1a,b and d. Targets of the selected diameter have a low complexity of experimental manufacturing, compared to large anodes, since the probability of defects forming in the seam decreases with a reduction of the brazed area. Prior to brazing, the graphite disks were dried at 1200 °C for 2 h in a vacuum in order to prevent desorption of residual gases during brazing. Additionally, the graphite parts had the triangular notches with a depth of 0.2 mm and a step of 0.5 mm to increase the joint area and the strength of the brazed seam (Fig. 1c). To study the evolution of the brazed seam microstructure and the mechanical properties of the molybdenum/graphite brazed joints, the samples in the form of a parallelepiped with a size of 10 × 10 mm and a height of 12 mm

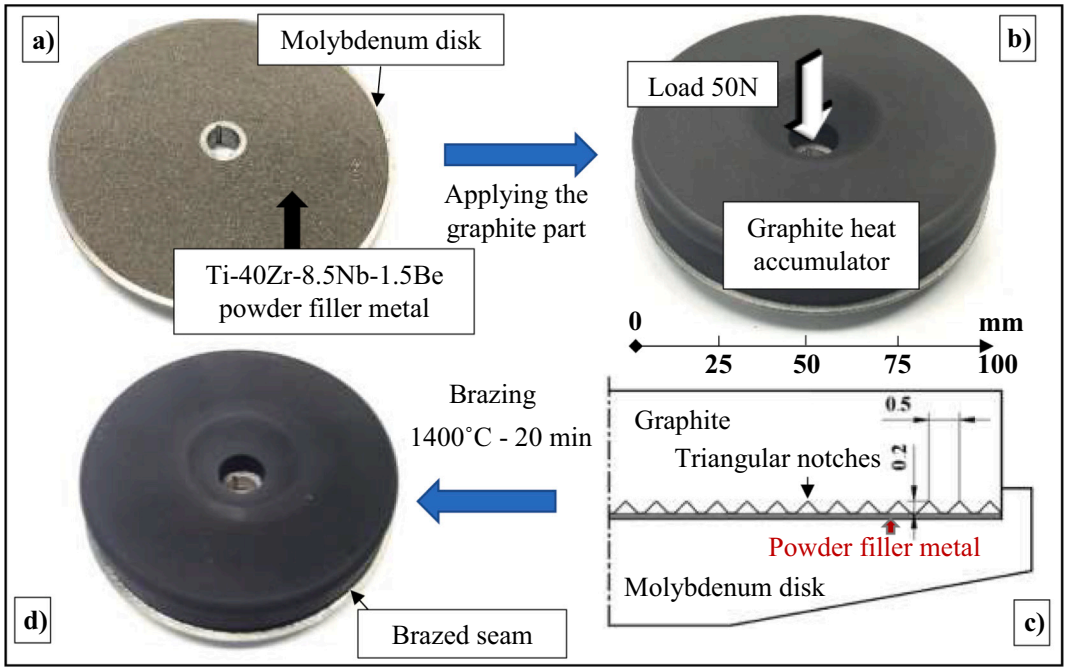

Fig. 1. Photo of 100 mm Mo/graphite X-ray target without (a) and with graphite part before brazing (b); Scheme of X-ray target brazing assembly (c); Brazed 100 mm molybdenum/graphite X-ray target (d).

obtained in the previous work were used [11].

The method of manufacturing Mo/graphite samples and X-ray targets was the same: brazing with powder filler metal Ti-40Zr-8.5Nb-1.5Be with a particle size of 50–350 μm at a temperature of 1400 °C with an exposure time of 20 min. The choice of a powder filler metal with a large particle size is associated with the the high reactivity of the filler metal components. A large particle powder (50–350 μm) has a relatively low specific surface, which reduces the chance of obtaining oxide inclusions in the brazed joint. Brazing was carried out in the Xerion XVAC1600 furnace with a heating speed of 20°/min, cooling – with the speed of the furnace, the residual pressure not higher than $6{\cdot}10^{-3}$ Pa. During the brazing, a load of 50 N was applied to the graphite disk in order to prevent the parts from shifting during brazing (Fig. 1b).

2.2. Simulation of the X-ray target working condition and a study of the Mo/graphite joint evolution

After brazing, the 100 mm anode was balanced on a Schenck pasio 15 balancing machine with further tests: 5 acceleration cycles up to 5000 rpm with a rotation of 1 min and a rapid stop for 2 s, while the 120 mm anode was subjected to simulated heating. Heating of the 120 mm anode and Mo/graphite joint samples was performed in AELTK-12 electron beam installation (accelerating Voltage 60 kV) in a vacuum of $\sim 10^{-3}$ Pa. A photo of the simulated heating preparation for the X-ray target and Mo/graphite samples is shown in Fig. 2.

The thermal load on the 120 mm X-ray target was chosen taking into account the exposure chart for the Varex G-2090Tri X-ray tube with an almost equal target size (127 mm) [25] and included: soft heating of the anode with a power of 3 kW of a continuous beam with an exposure of 10 min, followed by sequential thermal cycling: 10 kW – 30 s (3 cycles), 15 kW – 35 s (3 cycles) and 20 kW – 40 s (3 cycles). Between every cycle – 15 min break was made for radiation cooling of the target. The electron beam was applied to the surface of a molybdenum disk with a focal track diameter of 100 mm at a frequency of 150 revolutions per second and was created by the deflecting system of an electron gun (Fig. 2a), simulating the rotation of the anode. After simulated cyclic heating, the anode was cut by EDM (Electron-discharge machining) for the microstructural study and further vacuum annealing at a temperature of 1400 °C with an exposure of 2 h in order to simulate long-term operation.

Simulated «shock» heating of Mo/graphite samples was carried out, in order to imitate the most severe operating conditions of the anode brazed joint and study the evolution of brazed joint microstructure. To select the electron beam power with the chosen exposure time of 14 s., one of the samples had a thermocouple in the area of the brazed seam (Fig. 2b). Thermal cycling with an electron beam was carried out with various powers of the electron beam: 500, 600, 700 W. The experiment data showed that to simulate the temperature of the peripheral region of the X-ray target (temperature more than 1400 °C), an electron beam power of at least 600 W with an exposure of 14 s is required for a sample of such configuration (Fig. 2c). With the selected power, the remaining samples were heat-treated for 5, 10 and 20 cycles, as shown in Fig. 2d. The simulation of long-term operation conditions of the X-ray target was performed by annealing samples of the Mo/graphite joint at 1400 °C with exposure for 2 and 8 h in a vacuum furnace SSHVE-1.25/25. Summary data on operations with anodes and samples of the Mo/graphite joint is shown in Table 1.

2.3. Microstructure study and shear strength test

The microstructural study of brazed X-ray targets and Mo/graphite joint samples was made in a Carl Zeiss EVO 50 scanning electron microscope with an INCA X-act EDX microanalysis detector to identify the elements of the brazed seam. The phase composition of the brazed seam was determined with usage of diffraction patterns obtained by the "XSA" beamline of the Kurchatov synchrotron radiation source (wavelength $\lambda = 0.07930$ nm) [26]. The samples for XSA were a Mo/graphite joint plate with a thickness of 0.1 mm. Before structural analysis, the samples were annealed at 350 °C for 2 h in a vacuum furnace in order to reduce the internal stress induced by cutting and grinding. The shear strength test of the Mo/graphite brazed joint samples was performed in a special assembly on the Instron-5980 testing machine. The scheme of loading and testing of samples in the assembly is shown in the previous work [11].

3. Results and discussion

3.1. Microstructural analysis of a brazed X-ray target seam

After brazing, balancing and rotation test, the X-ray target with a diameter of 100 mm was applied to study the microstructure. The microstructure of the X-ray target fragments and the results of the EDX analysis of the seam phases are shown in Fig. 3 and Table 2.

The filler metal shows a good capability to fill the notches and infiltrate through the porosity of graphite to a depth of ~150 μm, providing a strong bond. According to Fig. 3, Table 2 and previous

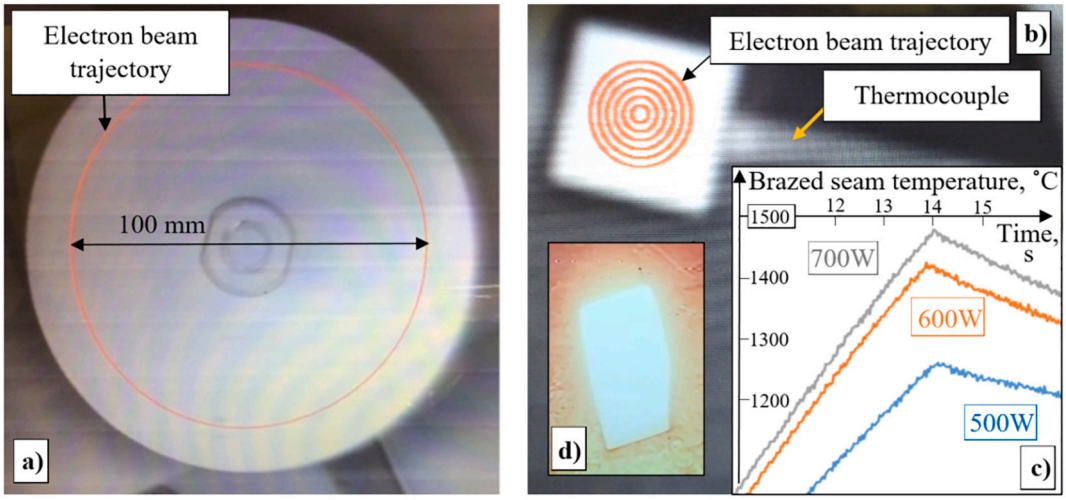

Fig. 2. Photos of the electron beam trajectory on a 120 mm Mo/graphite X-ray target (a); A Mo/graphite joint sample with an inserted thermocouple (b) and a temperature versus time chart during an electron beam exposure of different power (c); Sample of Mo/graphite brazed joint under simulated heating conditions at a beam power 600 W and 14 s exposure.

Table 1
Summary: operation with brazed X-ray targets and Mo/graphite joints.

Brazed anode/diameter			Mo/graphite brazed joint	
100 mm	120 mm		Thermal cycling (350 ↔ 1400 °C)/ amount of cycles	Annealing 1400 °C/ exposure, h
Balancing + rotation 5000 rpm (5 cycles)	Thermal cycling 3 kW (600 s), 10 kW (30s), 15 kW (35 s), 20 kW (40s)	Thermal cycling + annealing 1400 °C – 2 h	5 10 20	2 8

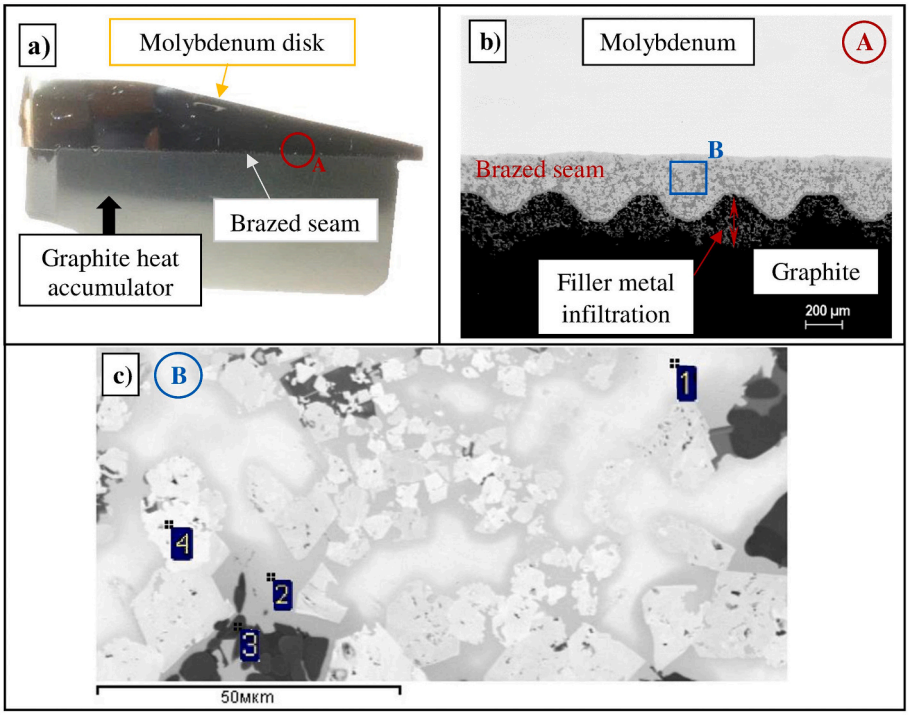

Fig. 3. Cross-section image of the 100 mm anode after brazing, balancing and EDM (a), the microstructure of the molybdenum disk/graphite accumulator joint at point A (b), the enlarged microstructure at point B (c).

Table 2
- Element composition of phases at points 1–4 from Fig. 3 in a Mo/graphite brazed joint.

Points	Atomic percentage of elements				
	C	Ti	Zr	Nb	Mo
1	0.0	61.3	4.5	7.0	27.2
2	0.0	75.7	6.8	6.0	11.5
3	51.4	41.7	5.8	1.1	0.0
4	39.3	6.7	51.9	2.1	0.0

research data at the work [11], the brazed seam visually consists of 3 phase: titanium carbide (Point 3), zirconium carbide (Point 4) and a β-(Ti,Mo) solid solution (Points 1 and 2). The distribution of molybdenum in the case of the brazed anode was not uniform: to the center of the Ti-Mo grain, its concentration was maximum (about 27.2%), while to the edge it decreased to 11.5%. The beryllides obtained in the previous study on the grain boundaries of the β-(Ti,Mo) solid solution were not visually detected. It is also worth noting that the distribution of carbides differs from that obtained earlier: in the anode seam, carbides crystallize to the entire depth of the brazed joint, preventing the formation of clear boundaries between Ti-Mo solid solution grains. Since in the previous research beryllides were formed only between the grains of the titanium-molybdenum solid solution, their absence may be related to the formation of the Be_2C phase, since the carbides have a uniform distribution in the seam. The titanium and zirconium carbides with the size around 5–20 μm located in matrix of the β-(Ti,Mo) solid solution. The obtained joint microstructure assumes high strength and high fracture toughness, as it is similar to a composite structure.

3.2. *Microstructure analysis of the X-ray target brazed joint after simulated heating*

Simulated thermal cycling of an anode with a diameter of 120 mm was carried out, in order to demonstrate the possibility of the brazed joint of X-ray target operate at high temperatures. During the exposure to an electron beam, the anode was strongly heated (Fig. 4).

After the simulated thermal cycling, the brazed joint maintained integrity and had no external defects. Due to the temperature gradient along the entire length of the brazed joint, it is most advisable to study the seam zone with the greatest thermal influence, closer to the peripheral zone of the Mo/graphite joint of the X-ray target. Molybdenum and graphite have different coefficients of thermal expansion (CTE). In addition, due to the temperature gradient, different expansion of the molybdenum disk and the graphite accumulator is possible. In this regard, the brazed joint can experience heavy loads, so cracks can form in the seam, which are aggravated by the presence of carbides. Cyclic heating of the anode will allow to find out whether the seam can resist

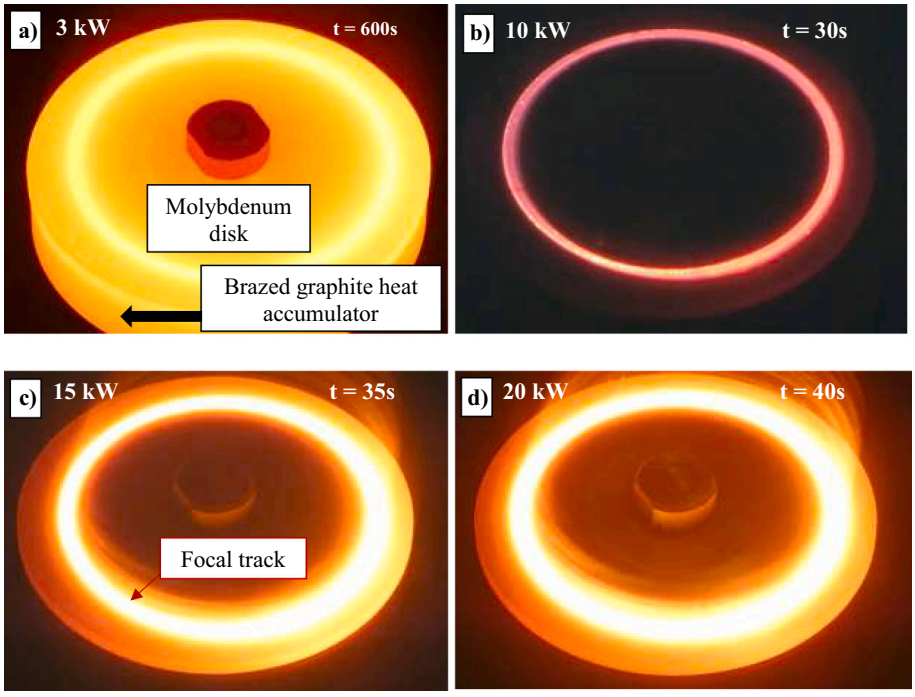

Fig. 4. Photos of an X-ray target during of electron beam exposure: a) 3 kW – 600 s; b) 10 kW – 30s; c) 15 kW – 35 s; d) 20 kW – 40s.

the development of cracks and how carbides affect the integrity of the seam. Fig. 5 shows the microstructure of the X-ray target brazed joint fragment after the simulated cyclic heating and after cyclic heating + annealing at 1400 °C with an exposure time of 2 h.

As can be seen from Fig. 5, the brazed joint has a rare porosity, probably due to releasing of residual gases from graphite during brazing. The microstructure of the joint remains stable and represents a matrix of the Ti-Mo alloy with inclusions of titanium and zirconium carbides, as before the application of thermal loads. The overwhelming size of the carbide inclusions after thermal cycling does not exceed 10 μm. After additional annealing at 1400 °C for 2 h of the anode fragment, the structure of the joint was preserved (Fig. 5c) and the size of the carbides inclusions did not change, but it was noticed that in the braze/graphite interface a structure called spinodal decomposition in the TiC-ZrC system is formed (Fig. 5d) [27], which indicates that mutual diffusion occurs in the carbide phases during prolonged exposure.

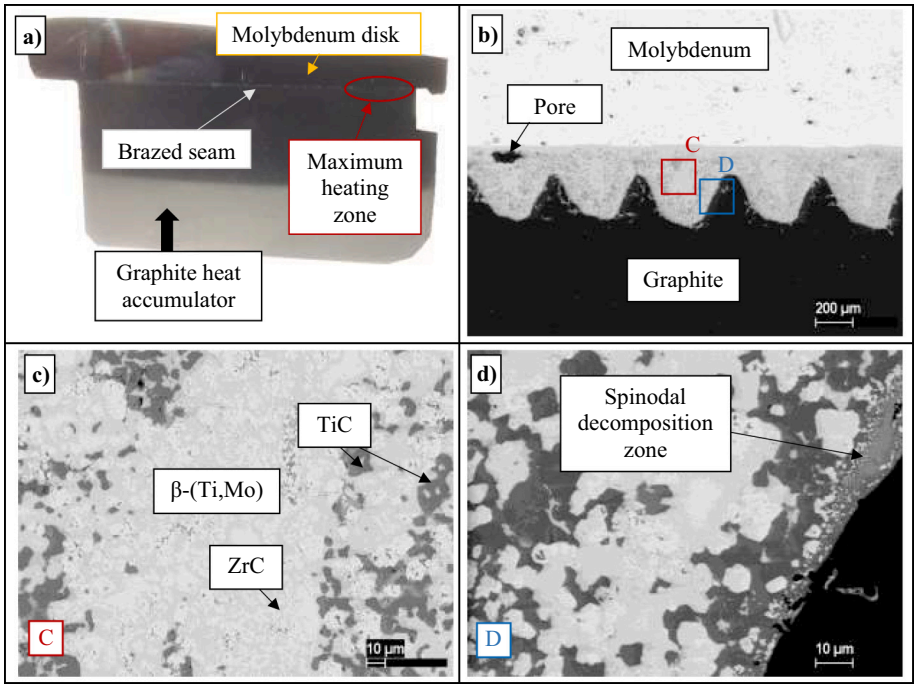

Fig. 5. The cross-section image of the 120 mm anode after brazing and imitation heating (a); microstructure of the molybdenum disk/graphite accumulator joint in the maximum heating zone after the simulated cyclic heating (b); enlarged microstructure at area C (c); microstructure of brazed joint after imitation cyclic heating + annealing 1400 °C – 2 h at area D (d).

3.3. Study of the Mo/graphite joint evolution during simulated heating

Since the peripheral zone of the X-ray target brazed joint is heated to a maximum temperature close to 1400–1500 °C during normal operation, the study of the microstructure and phase composition of the seam after thermal treatment is necessary in order to predict changes of its properties and evaluate its performance characteristics. The previous experiment on the anode showed the stability of the brazed seam structure, however, at maximum temperatures, the structure can change. Fig. 6 shows the distribution of elements in the seam after simulated cyclic heating (350 ↔ 1400 °C).

As can be seen from Fig. 6a, the seam initially has a heterogeneous structure with a predominant concentration of titanium near graphite, while zirconium is present in the center of the brazed seam. Both titanium and zirconium may indicate where the carbide phases are located, since EDX have a low sensitivity to carbon. Grains of the β-(Ti,Mo) solid solution are present throughout the entire brazed joint zone. However, after the simulated cyclic heating, a redistribution of components is observed: the elements are more evenly located inside the seam, reaching almost uniform distribution after 20 heating cycles (Fig. 6d). The size of each phase decreases, and the carbides infiltrate the entire depth of the seam, which leads to the formation of a structure with a β-(Ti,Mo) solid solution matrix with carbide inclusions. This redistribution of components may indicates the process of the brazed seam fragments secondary melting. The mechanism of beryllium influence on the eutectic crystallization of the molybdenum/graphite joint during brazing is described in detail in the previous work [11]. Under simulated heating conditions, the reverse process of eutectic melting is observed: as can be seen in the Mo-Be and Ti-Be phase diagram, there is a eutectic reaction at the Mo and Ti corner [28,29]. Based on this, a eutectic melt is likely to form in the Mo-Ti-Be triple system according to the following reaction (1):

$$\beta - (\mathrm{Ti, Mo}) + (\mathrm{TiBe_2, MoBe_2}) \rightarrow \mathrm{L} \quad (1)$$

which leads to the appearance of a liquid near the junction zone between beryllides and a β-(Ti,Mo) solid solution. If this liquid has a connection to graphite/carbides, then dissolution of carbon may occur in it, and carbides may form during cooling of the joint. The illustration of described process shown in Fig. 7.

In this repeated process of melting and solidification, more dispersed phases appear and the elements are evenly distributed inside the seam due to the rapid cooling of the sample, as can be seen in Fig. 7b,d. Thus, the partial melting of the seam is a mechanism of the phases dispersion in brazed joints at operating temperatures above the melting point of the ($TiBe_2$, $MoBe_2$) + β-(Ti,Mo) eutectic.

The liquid in the joint can be the reason of the degradation of its mechanical properties during high-temperature application, so the study of the evolution of the phase composition during the operation of the X-ray target becomes an important issue. The long-term thermal annealing (1400 °C and 8 h) demonstrates a slightly different structure of the brazed joint (Fig. 8).

As can be seen from Fig. 8a,b, when comparing the thermally untreated microstructure, the amount of titanium carbide in the brazed joint increases significantly, and the size of the β-(Ti,Mo) solid solution grains decreases. At the same time, it should be noted that the content of molybdenum in β-(Ti,Mo) is higher than in the joint after brazing, and reaches 47 at. % (Table 3). This increase leads to an increase in the temperature of the solidus and liquidus of the β-(Ti,Mo) solid solution,

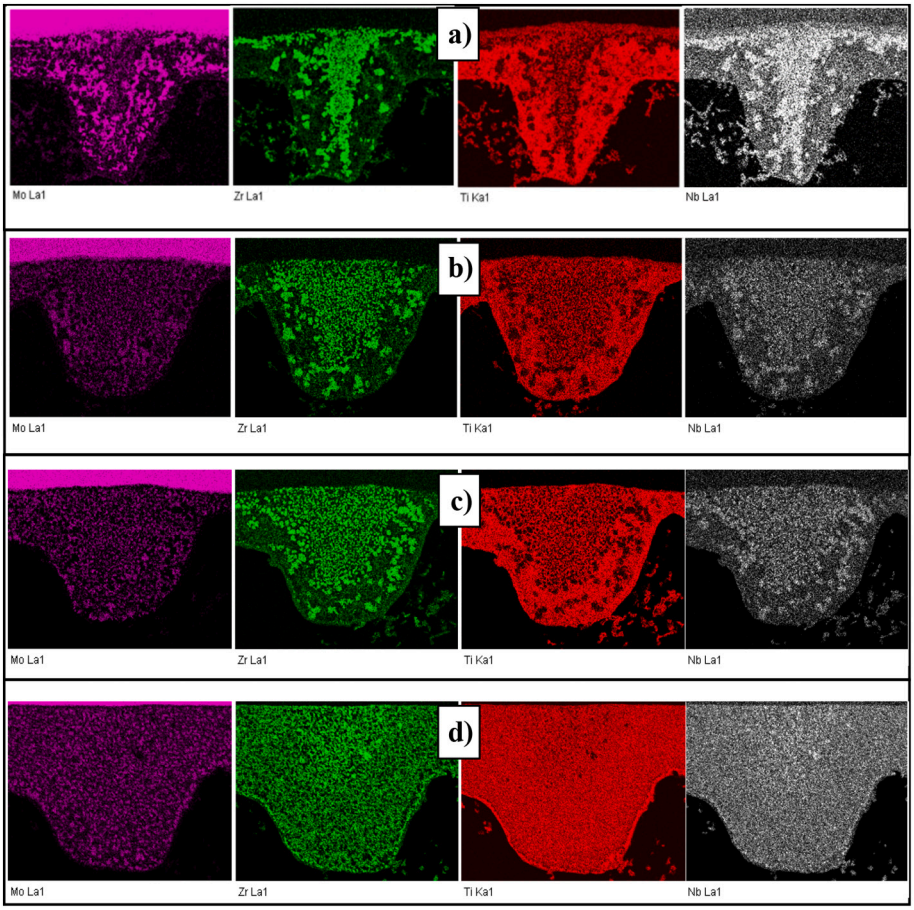

Fig. 6. Element mapping of the Mo/graphite brazed joint sample: a) initial distribution; b–d) 5, 10 and 20 cycles of the simulated heating from 350 °C to a 1400 °C, respectively.

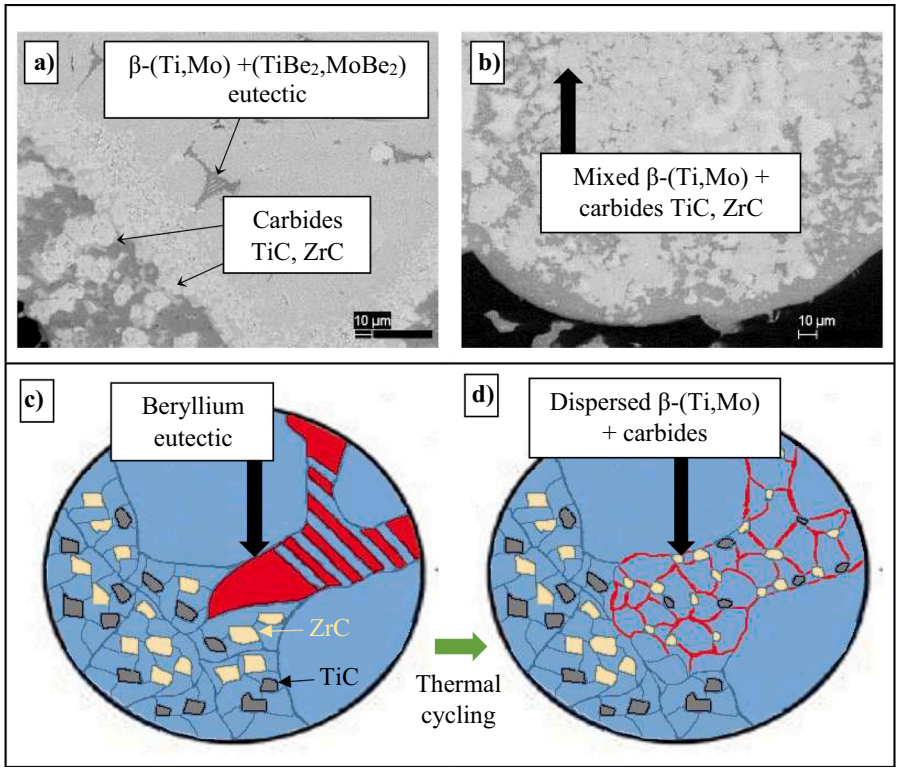

Fig. 7. Illustration of the recrystallization process in the brazed seam during the simulated cyclic heating: a,c) initial microstructure; b,d) microstructure after 20 cycles (350 ↔ 1400 °C) of the simulated heating.

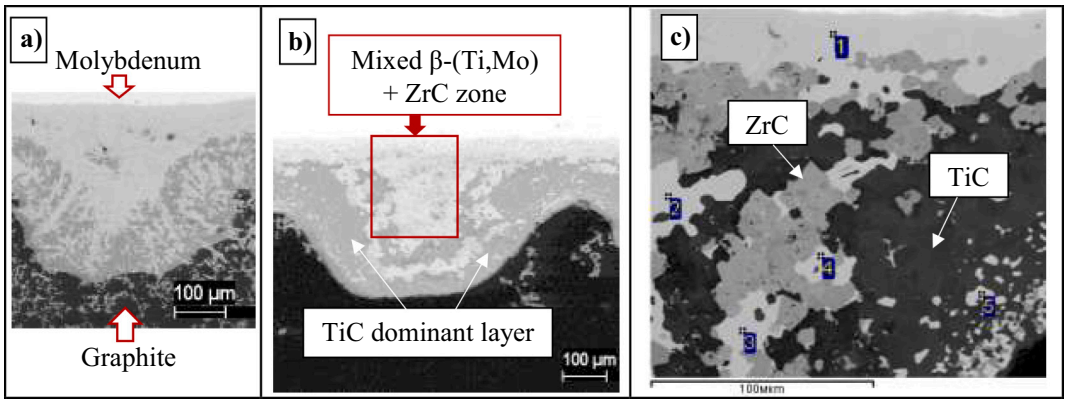

Fig. 8. SEM micrographs of the Mo/graphite brazed joint: a) microstructure of the Mo/graphite joint before annealing; b) General view of the joint microstructure after annealing 1400 °C – 8 h; c) enlarged fragment of seam from b).

Table 3
Element composition of phases at points 1–4 from Fig. 7 in a Mo/graphite brazed joint.

Points	Atomic percentage of elements			
	Ti	Zr	Nb	Mo
1	45.6	2.2	6.1	46.1
2	46.5	2.3	6.5	44.7
3	46.4	2.2	6.0	45.4
4	45.9	2.1	6.0	46.0
5	44.9	2.2	5.9	47.0

which favorably affects the heat resistance of the seam and is suitable for high-temperature use.

To study the change in the phase composition of the joint, X-ray spectra for Mo/graphite brazed joints after 20 heating cycles of 350 ↔ 1400 °C and vacuum annealing of 1400 °C – 8 h were obtained (Fig. 9).

The analysis of the diffraction pattern showed that after 20 cycles of heating (350 ↔ 1400 °C), the qualitative composition of the brazed seam does not change and includes: titanium carbide (TiC), zirconium carbide (ZrC), a β-(Ti,Mo) solid solution and beryllides ($TiBe_2$, $MoBe_2$). However, after heat treatment at a temperature of 1400 °C with an exposure of 8 h, the phase composition of the seam changes, and the peaks responsible for beryllides disappear. Thus, it has been established that under conditions of prolonged annealing, due to the diffusion of carbon in the brazed seam, the crystallization of titanium and molybdenum beryllides is suppressed, which transforms the joint into a refractory state. During the crystallization of the refractory Ti-Mo phase and carbides, the appearance of a liquid during thermal cycling is impossible,

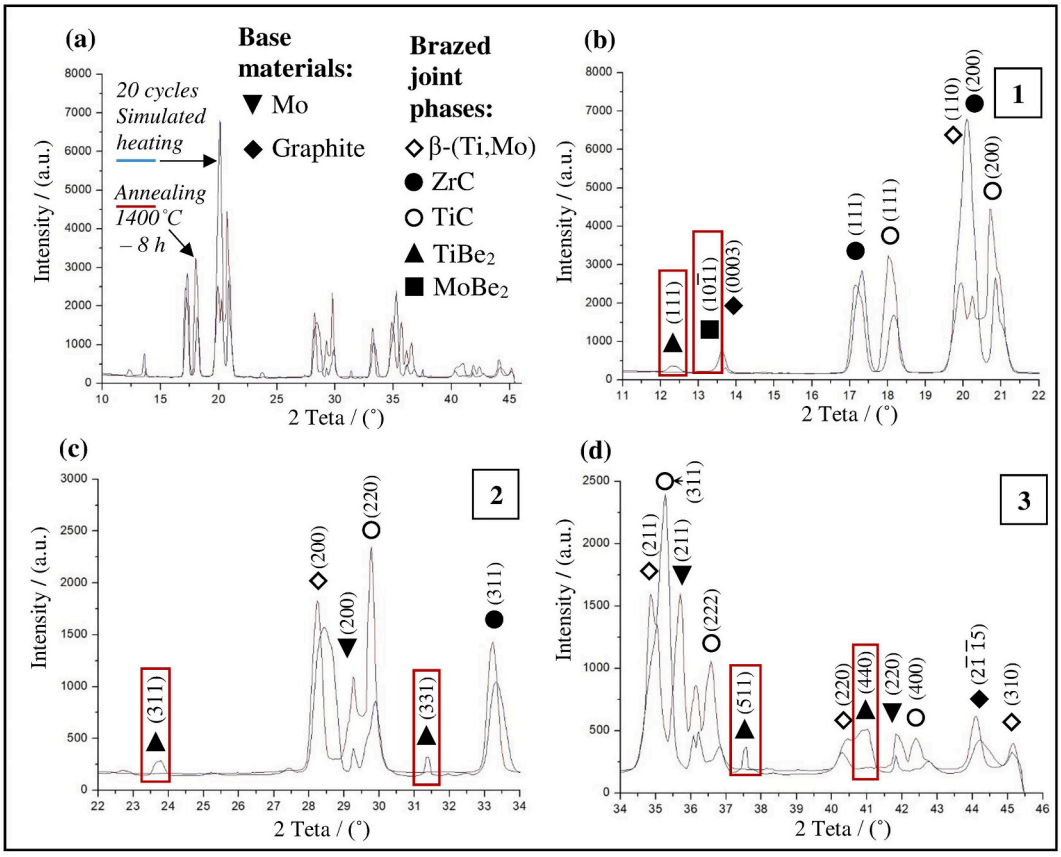

Fig. 9. Diffraction pattern of the Mo/graphite brazed joint (a) and magnified images of the pattern parts (b–d) encircled by rectangles 1–3; (the highlighted lines correspond to beryllides).

since carbides have high melting points, as well as a β-(Ti,Mo) solid solution. The absence of beryllides has a positive effect on the thermal stability of the joint, but a high carbide content in the joint can reduce the strength of the seam, since they are very brittle. In the case of arising thermal stresses due to the rapid heating of the X-ray target periphery, the cracking of the seam may happen. Therefore, the mechanical strength test of thermally threated joints must be carried out.

3.4. Mechanical properties of the thermally treated Mo/graphite joint

Due to the rotation of the X-ray target, the loads occur in the brazed seam. Changes in the microstructure of the joint due to carbon diffusion/growth of carbides can embrittle it and significantly reduce its mechanical characteristics. This can lead to the detachment of the graphite heat accumulator and failure of the anode. The destruction of the target during operation is unacceptable, as it can lead to damage to the X-ray tube and the surrounding equipment. Therefore, mechanical shear strength tests was carried out for brazed molybdenum/graphite joints with different heat treatment. The results of the average shear strength of the molybdenum-graphite brazed joint are shown in Table 4, as well as the typical sample image and microstructure of the seam after the sample failure is shown in Fig. 10.

As can be seen from Fig. 10, the failure of the sample occurred as follows: the cracking starts in the graphite, then the crack spreads to the tops of the notches and then parallel to the brazed joint (Fig. 10b). The failure leads to the formation of a thin layer of graphite above the brazed seam (Fig. 10a). After mechanical tests, the cracks perpendicular to the joints were also found in the seam (Fig. 10b). The cracking occurred in the carbide layer of the joint, while the Ti-Mo solid solution effectively resisted its growth. Such cracks may indicate the presence of perpendicular tensile stresses in the joint due to the temperatures gradient and mismatch in CTE of graphite and molybdenum.

The picture of Mo/graphite samples failure indicates that the strength of the joint after the considered heat treatments is higher than the strength of graphite, and the crack propagation in the seam itself is the least energy-efficient than in graphite. Previously, it was shown that the filler metal infiltrates to a graphite at the depth of about 150 μm. In these infiltrates, most likely, the formation of titanium/zirconium carbides occurs. Since the CTE of graphite and titanium/zirconium carbides is not equal, stresses may occur during cyclic heating/cooling due to volumetric changes, which apparently lead to the formation of microcracks in the graphite and loss of strength in the layer close to the brazed seam. Thus, the change in the microstructure of the brazed joint during the selected thermal treatment does not lead to a significant degradation of the joint mechanical properties. Instead, there is a deterioration in the mechanical properties of graphite in the near-surface layer to the seam. In this case, it is necessary to avoid high open porosity and prevent deep penetration of the filler metal into the graphite, since this will lead to

Table 4
Average shear strength of the Mo/graphite joint.

Heat treatment	After brazing [11]	Thermal cycling: 350↔1400 °C/number of cycles			Vacuum annealing, h	
		5	10	20	2	8
Average shear strength, MPa	28.0 ± 0.9	24.6 ± 2.4	25.2 ± 2.1	23.4 ± 2.5	26.6 ± 2.6	26.1 ± 6.4

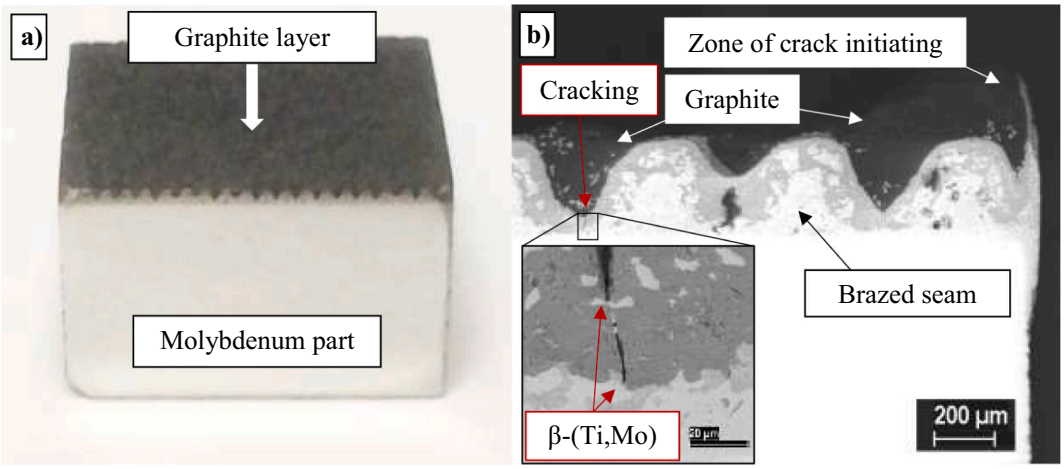

Fig. 10. Cross-section image of the Mo/graphite joint sample after the shear strength test (a), the microstructure of the brazed seam after the shear strength test (heat treatment: 1400 °C – 8 h.) (b), the enlarged microstructure of the joint with a crack (c).

softening of graphite during thermal cycling.

4. Conclusions

1. The brazing of the two X-ray targets with a diameter of 100 and 120 mm was successfully carried out. The resulting brazed joint between the molybdenum disk and the graphite heat accumulator consists of a matrix of a Ti-Mo solid solution with incursions of zirconium and titanium carbides. Under operating conditions within a short cycle of operation and at a constant temperature of 1400 °C with a holding time of 2 h, the joint maintains integrity and microstructural stability.
2. The evolution of the brazed molybdenum/graphite joint at the maximum operating temperature is studied. Thermal cycling (350 °C ↔ 1400 °C) of the brazed Mo/graphite joint revealed that partial melting of beryllium eutectic occurs in the seam, leading to recrystallization and fragmentation of the structural components of the joint. The exposure at a temperature of 1400 °C for 8 h provokes a significant increase in the amount of titanium carbides, rising the concentration of molybdenum in a β-(Ti, Mo) solid solution and the degeneration of beryllides from the seam, which turns the joint into a refractory state.
3. Shear tests showed that the strength of the Mo/graphite joint remains at the minimum level of 23.4 ± 2.5 MPa (after 20 cycles of heating 350 ↔ 1400 °C) and 26.1 ± 6.4 MPa (after vacuum annealing of 1400 °C – 8 h). The destruction of the Mo/graphite joint occurred by cracking the graphite with the growth of a crack in the tops of the seam notches parallel to the seam. The main reason for a graphite failure is seems to be the formation of microcracks, due to the infiltration of the filler metal into the open porosity of graphite under the influence of capillary forces and the discrepancy in the CTE of graphite and titanium/zirconium carbides.

Funding

This work was supported by the MEPhI Academic Excellence Project.

Declaration of competing interest

The authors declare that they have no known competing financial interests or personal relationships that could have appeared to influence the work reported in this paper.

Acknowledgements

The authors are grateful to the National Research University "Moscow Power Engineering Institute" for using the AELTK-12 installation for thermal testing of a brazed X-ray target.

Appendix A. Supplementary data

Supplementary data to this article can be found online at https://doi.org/10.1016/j.jmapro.2021.07.035.

References

[1] Behling R. Modern diagnostic X-ray sources. London: CRC Press, Taylor and Francis Group; 2016. https://doi.org/10.1201/b18655.
[2] Mirski Z. Brazing a graphite composite to molybdenum alloy TZM using active copper-based filler metals with chromium additive. Arch Metall Mater 2011;56:829–37. https://doi.org/10.2478/v10172-011-0092-y.
[3] Smid II, Kny E, Kneringer G, Reheis N. Influence of cyclic thermal loading on brazed composites for fusion applications. J Nucl Mater 1990;171:165–71. https://doi.org/10.1016/0022-3115(90)90362-Q.
[4] Wen Y, Chen W, Ding B. Diffusion Welding Interface Reaction Analysis of Molybdenum and Graphite. 2011.
[5] Dong L, Chen W, Hou L, Wang J, Song J. Metallurgical and mechanical examinations of molybdenum/graphite joints by vacuum arc pressure brazing using Ti-Zr filler materials. J Mater Process Technol 2017;249:39–45. https://doi.org/10.1016/j.jmatprotec.2017.06.007.
[6] Smid I, Croessmann CD, Salmonson JC. Brazed graphite/refractory protection elements metal composites for first-wall. J Nucl Mater 1991. https://doi.org/10.1016/0022-3115(91)90053-A.
[7] Traxler H, Arnold W, Knabl W, Rödhammer P. Non-destructive evaluation of brazed joints by means of acoustic emission. J Acoust Emiss 2003;20:257–64.
[8] Wang KS, Tan JF, Hu P, Yu ZT, Yang F, Hu BL, et al. La_2O_3 effects on TZM alloy recovery, recrystallization and mechanical properties. Mater Sci Eng A 2015;636:415–20. https://doi.org/10.1016/j.msea.2015.03.114.
[9] Primig S, Leitner H, Clemens H, Lorich A, Knabl W, Stickler R. On the recrystallization behavior of technically pure molybdenum. Int J Refract Met Hard Mater 2010;28:703–8. https://doi.org/10.1016/j.ijrmhm.2010.03.006.
[10] Warren JM. Patent USOO6421423B1 - Two-step Brazed X-ray Target Assembly. 2002.
[11] Fedotov I, Suchkov A, Sliva A, Dzhumaev P, Kozlov I, Svetogorov R, et al. Study of the microstructure and thermomechanical properties of Mo/graphite joint brazed with Ti–Zr–Nb–Be powder filler metal. J Mater Sci 2021;56:11557–68. https://doi.org/10.1007/s10853-021-06015-9.
[12] Bachurina D, Vorkel V, Suchkov A, Gurova J, Ivannikov A, Penyaz M, et al. Overview of the mechanical properties of tungsten/steel brazed joints for the demo fusion reactor. Metals (Basel) 2021;11:1–11. https://doi.org/10.3390/met11020209.
[13] Fedotov VT, Suchkov AN, Kalin BA, Sevryukov ON, Ivannikov AA. Stemet solders for brazing of modern technology materials. Tsvetnye Met 2014:32–7.
[14] Kalin BA, Suchkov AN, Fedotov VT, Sevryukov ON, Ivannikov AA, Mazul IV, et al. Application of Rapidly Quenched Ribbon-type Filler Metals for Brazing of the High-Heat-Flux Elements of ITER1055; 2017. https://doi.org/10.13182/FST12-A13381.
[15] Plankensteiner A, Rödhammer P. Finite element analysis of X-ray targets. Proc 15th Int Plansee Semin 2001:9–22.

[16] Kumar R, Ratnala SR, Veeresh Kumar GB, Shivakumar Gouda PS. Thermal analysis on x-ray tube for exhaust process. IOP Conf Ser Mater Sci Eng 2018:310. https://doi.org/10.1088/1757-899X/310/1/012162.
[17] Bachurina D, Suchkov A, Gurova J, Savelyev M, Dzhumaev P, Kozlov I, et al. Joining tungsten with steel for DEMO: simultaneous brazing by cu-Ti amorphous foils and heat treatment. Fusion Eng Des 2020. https://doi.org/10.1016/j.fusengdes.2020.112099.
[18] Bachurina D, Suchkov A, Kalin B, Sevriukov O, Fedotov I, Dzhumaev P, et al. Joining of tungsten with low-activation ferritic–martensitic steel and vanadium alloys for demo reactor. Nucl Mater Energy 2018;15:135–42. https://doi.org/10.1016/j.nme.2018.03.010.
[19] Penyaz MA, Ivannikov AA, Kalin BA, Dzhumaev PS. Thermal fatigue damage of steel joints brazed with various nickel filler metals. Non-Ferrous Met 2019;46:33–9. https://doi.org/10.17580/nfm.2019.01.06.
[20] Dandapat N, Ghosh S, Guha BK, Datta S, Balla VK. Effect of processing parameters on thermal cycling behavior of Al_2O_3-Al_2O_3 brazed joints. Metall Mater Trans B Process Metall Mater Process Sci 2016;47:2946–53. https://doi.org/10.1007/s11663-016-0731-9.
[21] Dandapat N, Ghosh S, Pal KS, Datta S, Guha BK. Thermal cycling behavior of alumina-graphite brazed joints in electron tube applications. Trans Nonferrous Met Soc China (English Ed) 2014;24:1666–73. https://doi.org/10.1016/S1003-6326(14)63239-8.
[22] Tang M, Chen W, Liu Y. Analysis of the brazing joints of tubular zirconia ceramics and 06Cr19Ni10 stainless steel tubes. Adv Appl Ceram 2021;120:10–6. https://doi.org/10.1080/17436753.2020.1840265.
[23] Stankus SV, Savchenko IV, Agadzhanov AS, Yatsuk OS, Zhmurikov EI. Thermophysical properties of MPG-6 graphite. High Temp 2013;51:179–82. https://doi.org/10.1134/S0018151X13010173.
[24] Stankus SV, Yatsuk OS, Zhmurikov EI, Tecchio L. Thermal expansion of artificial graphites in the temperature range 293–1650 K. Thermophys Aeromechanics 2012;19:463–8. https://doi.org/10.1134/S0869864312030110.
[25] Varex Imaging. Rotating anode X-ray tube G-2090TRI. In: Product description. Varex Imaging; 2017.
[26] Svetogorov RD, Dorovatovskii PV, Lazarenko VA. Belok/XSA diffraction beamline for studying crystalline samples at Kurchatov synchrotron radiation source. Cryst Res Technol 2020;55:1–6. https://doi.org/10.1002/crat.201900184.
[27] Li Y, Katsui H, Goto T. Phase decomposition of TiC-ZrC solid solution prepared by spark plasma sintering. Ceram Int 2015;41:14258–62. https://doi.org/10.1016/j.ceramint.2015.07.055.
[28] Tokunaga T, Ohtani H, Hasebe M, Nakashima K. Thermodynamic analysis of the Be-Mo binary phase diagram. J Japan Inst Met Mater 2007;71:187–9. https://doi.org/10.2320/jinstmet.71.187.
[29] Tokunaga T, Ohtani H, Hasebe M. Thermodynamic evaluation of the phase equilibria and glass-forming ability of the Ti-Be system. J Phase Equilib Diffus 2006;27:83–91. https://doi.org/10.1361/105497106X92844.